Classification of Forest Species using Hyperspectral Imaging Techniques

Ramesh Bhatta
Rochester Institute of Technology

***Abstract*—Species level classification is an important remote sensing application to forest monitoring and resource management. Hyperspectral imagery based classification leverages the rich spectral information collected across multiple narrow, contiguous wavelength bands to distinguish vegetation types based on their unique spectral signatures. Unlike RGB or multispectral data, hyperspectral imagery has a potential to provide fine details on plant biochemical and structural properties, enabling accurate species classification, even those with subtle differences. We exploited a 36 bands hyperspectral imagery collected using CASI airborne sensor over a forested region to classify four species classes- *Eucalyptus grandis (Gran)*, *Eucalyptus dunnii (Dun)*, *Eucalyptus grandis x nitens (GraNit)*, *Acacia mearnsii (Amea)* along with other two classes- *OtherTree* and *Bare Soil (BS)*. Maximum Likelihood Estimation (MLE) was used in raw data and also in Minimum Noise Fraction (MNF) based dimension reduced data for classification. An overall accuracy of 70.01% and Kappa Coefficient of 63.11% was obtained when using raw data, while a slight improvement in the accuracy of 71.28% and kappa coefficient of 64.55% was obtained while using MNF based data. Using the raw data the highest producer's accuracy (97.67%) and user's accuracy (93.33%) was obtained for *Bare Soil* while lowest producer's accuracy (36.96%) and user's accuracy (49.16%) was obtained for *OtherTree* class. Same trend is also seen with MNF reduced data, with a slight improvement in classification: *Bare Soil* (producer: 98.29%, user: 94.63%) and *OtherTree* (producer: 39.72%, user: 55.18%). All other species were classified with an acceptable margin in terms of accuracy range (Raw-producer: 46.26% for *Gran* to 95.18% for *Amea*, Raw-user: 61.13% for *Gran* to 84.97% for *Amea*, MNF-producer: 48.30% for *Gran* to 96.12% for *Amea*, MNF-user: 63.42% for *Gran* to 87.96% for *Amea*). Thus, a simple hyperspectral-based approach demonstrates significant potential for species-level classification, offering a powerful solution to an otherwise challenging problem.**

***Index Terms*—Hyperspectral, Classification, Supervised, Maximum Likelihood Estimation, Minimum Noise Fraction (MNF), Producer's Accuracy, User's Accuracy.**

I. Introduction

TREE species identification and classification through the use of remote sensing methods provides an efficient and economical mean of monitoring and sustainably managing forest inventory and resources [1]. Such methods are widely used in the literatures and also in the real world application for tree species classification and forest studies in different ecological systems. Multiple remote sensing modalities like Spectral (*Multispectral [2]* and *Hyperspectral [3]*), Structural (*LiDAR [4]*), and sometimes SAR (*Synthetic Aperture Radar [5]*) have been used in these classifications routines. Multispectral imagery contains fewer, discrete broadband channels and are mostly used for land cover classifications or sometimes forest type identification. To increase the accuracy of classification using multispectral imagery they are occasionally supplemented with structural information obtained from LiDAR [6]. SAR usage in individual species classification is rare due to the problem of information blending in backscatter coefficients. This means in dense or mixed forests, radar waves interact and reflect off multiple surfaces before reaching to the sensor which leads to recording of mixture of signal from multiple species and make it difficult for class seperatibility of the species. However studies show that fusion of SAR with spectral features can result in high classification accuracy [7]. On the other hand hyperspectral imagery shows a huge potential to be a standalone modality for species level classification due to its ability to record the spectral response from individual species using continuous narrow bands with high sampling and spectral resolution. Such detailed information from hyperspectral data allows for the distinction of minute spectral variations among the tree species [8]. In terms of information content, hyperspectral imagery can provide more accurate and detailed information extraction compared to any other remotely sensed data. Thus, data rich hyperspectral imagery has potential to capture even the slightest variations in the species spectral signatures which multispectral imagery fail to do and can hence increase the quality of classification. However such information rich hyperspectral system comes at a cost- higher operational cost during data collection and higher computational cost during product generation. Also the complexity of the system itself increases while going from multisepctral to hyperspectral systems and hence these data are not often readily available as multispectral systems. With all these consideration hyperspecral system are usually available in airborne and satellite platforms and are generally used for large scale (landscape level) species classifications.

The high amount of band information present in the hyperspectral data poses a problem that increase in band data increases the number of required training samples exponentially for maintaining classification accuracy [9]. This requires for using a suitable dimensionality reduction techniques for training of classification algorithm. One common technique for band data reduction in hyperspectral imagery for classification is Minimum Noise Fraction (MNF) [10]. The Minimum Noise Fraction (MNF) transformation is a two-step process involving principal component analysis (PCA). First, it applies PCA to reduce correlations in noisy data, effectively separating noise from the signal. Then, the denoised principal components are used to perform the final transformation, enhancing the representation of essential image features. The MNF transformed bands are now ranked based on their importance/variability determined by the eigen-values from highest to lowest. These MNF bands can be subsetted to a few bands for training a classifier. In this paper we work on classifying four species classes- *Eucalyptus grandis (Gran)*, *Eucalyptus dunnii (Dun)*, *Eucalyptus grandis x nitens (GraNit)*, *Acacia mearnsii (Amea)* along with other two classes- *OtherTree* and *Bare Soil (BS)* using data collected from a 36 bands Compact Airborne Spectrographic Imager (CASI) hyperspectral system over a forested ecosystem. These tree species are selected for classification due to their vital ecological role in the region. We used a simple yet elegant classification algorithm namely: Maximum Likelihood Estimation (MLE) [11] towards fulfilling our objectives: 1) Classification of tree species using raw hyperspectral data and reduced MNF bands and 2) Comparison of perfomance of MLE with Spectral Angle Mapper (SAM) [12] classification algorithm. These tasks were designed based on the ecological, system and algorithm utility considerations required for species classification in those regions.

II. DATA AND METHOD

The data collected for this work contains a 36 band hyperspectral imagery with a spatial resoultion of 1m collected over forested region. The CIR (colour-infrared) composite NIR, red, and green band) plot of the location with the labeled training sample pixels is shown in the Figure 1.

We used Maximum likelihood estimation method (MLE) on the data for classification. MLE finds the parameter θ that maximizes the probability of observed data. Given a dataset $\mathcal{D} = \{(\mathbf{x}_i, y_i)\}_{i=1}^{N}$, the likelihood function is:

$$L(\theta) = \prod_{i=1}^{N} P(y_i|\mathbf{x}_i, \theta)$$

Taking the logarithm simplifies it:

$$\log L(\theta) = \sum_{i=1}^{N} \log P(y_i|\mathbf{x}_i, \theta)$$

For classification, $P(y_i|\mathbf{x}_i, \theta)$ is often modeled using a function like softmax [13]:

$$P(y_i = k|\mathbf{x}_i, \theta) = \frac{\exp(\theta_k^T \mathbf{x}_i)}{\sum_{j=1}^{K} \exp(\theta_j^T \mathbf{x}_i)}$$

The goal is to find θ^* that maximizes $\log L(\theta)$, typically solved using gradient-based optimization.

We applied MLE for classification in both original raw data as well as dimension reduced data. The MNF transformation reduces dimensionality by capturing essential information within a smaller number of bands. The first 2 MNF bands are shown in Figure 2. Analysis of MNF reduced bands shows that Band 1 captures the flight lines information in which appears a diagonal stripes in the band image. Band 2 captures information regarding soil content in the imagery and so on. These MNF bands represent unique information content of the imagery in reduced dimensions. Similarly after band 10 everything is almost noise, so these bands can be rejected during analysis.

Fig. 1: Hyperspectral data collected over forested area with training classes.
Red: GraNit, Blue: Gran, cyan: BS, Teal: Dun, Pastel-Red: Amea

Also we can see from the Figure 1 that compared to number of pixels present in the scene, we have a small number of sample for training the classification algorithm. With higher dimension data this poses insufficient training data problem. So before using the data in classification we resized the bands in both raw data and MNF reduced data space using *Stepwise Discriminant Analysis* method. The following bands were found relevant in each data space:

- Raw Radiance (N=13): **B9, B11, B17, B5, B20, B31, B18, B19, B35, B23, B21, B14, B1**
- MNF Space (N=15): **B3, B6, B13, B8, B2, B9, B10, B11, B14, B1, B16, B4, B17, B18, B5**

These bands represent most informative spectral bands for

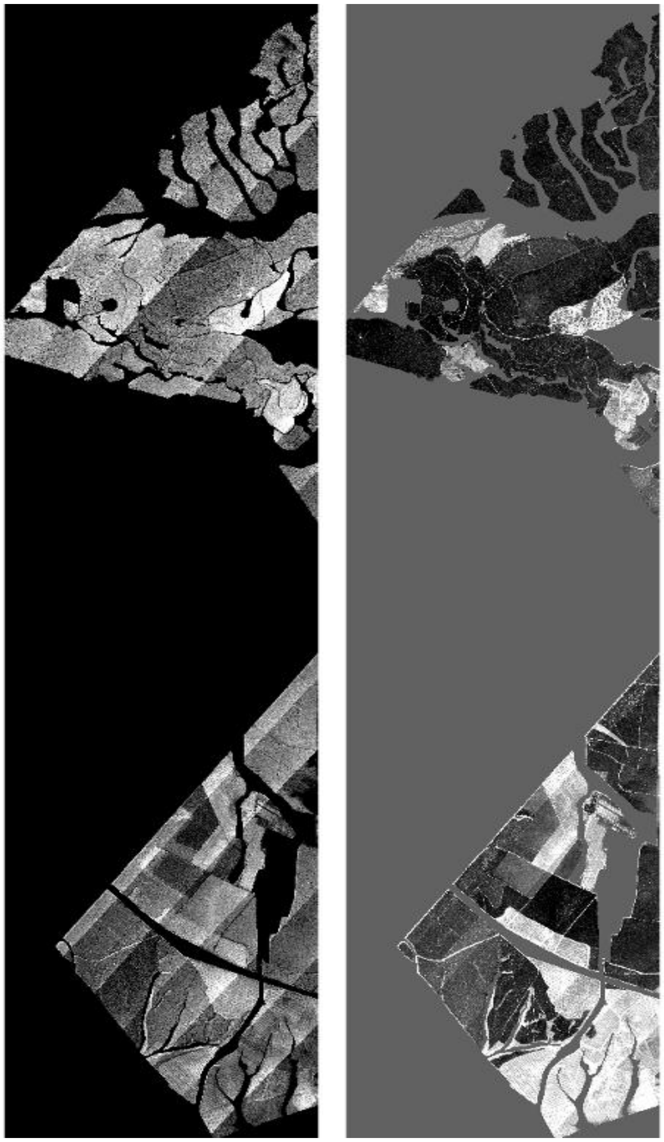

Fig. 2: MNF Bands: Band 1 (left) and Band 2 (right)

distinguishing different classes of the imagery. So these sets of bands were applied our classification algorithm and the results are presented in section below.

III. RESULTS

A. CLASSIFICATION OUTCOME

The results for supervised classification based on MLE on both band resized raw and MNF reduced data is shown in the Figure 3. From figure we can see that overall outcome of classification at such larger scale is quite good. The pixels around the training samples are mostly classified correctly with some confusion at the transition boundaries between species dominated regions which can be seen on the northern part of the image. In general the results are not much different for both raw data based and MNF based classification, however MNF based result have a comparative sharper boundaries in classified image with less mixed classification regions indicating a lesser amount of noise. Section below presents the comparative analysis of result performance for both classifications.

B. CLASSIFICATION STATISTICS

Table I shows the overall outcome statistics for the classification. An overall accuracy of 70.01% and Kappa Coefficient of 63.11% was obtained when using raw data, while a slight improvement in the accuracy of 71.28% and kappa coefficient of 64.55% was obtained while using MNF based data. Using the raw data the highest producer's accuracy (97.67%) and user's accuracy (93.33%) was obtained for *Bare Soil* while lowest producer's accuracy (36.96%) and user's accuracy (49.16%) was obtained for *OtherTree* class. Same trend is also seen with MNF reduced data, with a slight improvement in classification: *Bare Soil* (producer's: 98.29%, user's: 94.63%) and *OtherTree* (producer's: 39.72%, user's: 55.18%). All other species were classified with an acceptable margin in terms of accuracy range (Raw-producer's: 46.26% for *Gran* to 95.18% for *Amea*, Raw-user's: 61.13% for *Gran* to 84.97% for *Amea*, MNF-producer: 48.30% for *Gran* to 96.12% for *Amea*, MNF-user's: 63.42% for *Gran* to 87.96% for *Amea*). The highest accuracy and lowest confusion for the *Bare Soil* class can be attributed to the fact that Bare Soil have a very different spectrum compared to a vegetation spectrum which makes it easily separable by the algorithm. Similarly, the lowest accuracy and highest confusion for the *OtherTree* class is due to its close resemblance with other vegetation spectra. These inferences can also be made from the confusion matrix (not included here). Also since *GranNit: Eucalyptus grandis x nitens* is the hybrid of *Gran: Eucalyptus grandis*, these two classes has highest confusion during classification and hence the relatively lower accuracy for *Gran* class.

C. ENVI SPECTRAL HOURGLASS SAM BASED CLASSIFICATION

We ran the same classification using an automatic ENVI spectral hourglass tool. This tool works by first transforming the raw data into MNF space and selecting the most important MNF bands, then using *Pixel Purity Index (PPI)* algorithm [14] to find pure end-member pixels. After determining the end-members the classification algorithm-Spectral Angle Mapper (SAM) is used to classify all the pixels in the data.

From the analysis of eigen-variability we choose the number of MNF bands to keep for classification. From figure Figure 4 we can see that almost drops almost to 0 which means that 10 MNF bands are enough for explaining most of the variability in the data. So we use the first ten bands for classification. After that we ran the PPI algorithm for endmember determination and found that based on the data the algorithm determined 11 pure pixels in the scene. The collection of spectra for the determined end members is shown in Figure 5.

We can see that there are some vegetation spectra with the distinct red-edge characteristics. These could be the different type of species we are interested in based on the knoweldge of vegetation in that area. Other spectra resemble with different type of soil spectrum (different level of wetness). A flat spectrum resembling water is also identified as end member pixel by the algorithm. These end member were fed into SAM algorithm for classification and the result is shown in Figure 6.

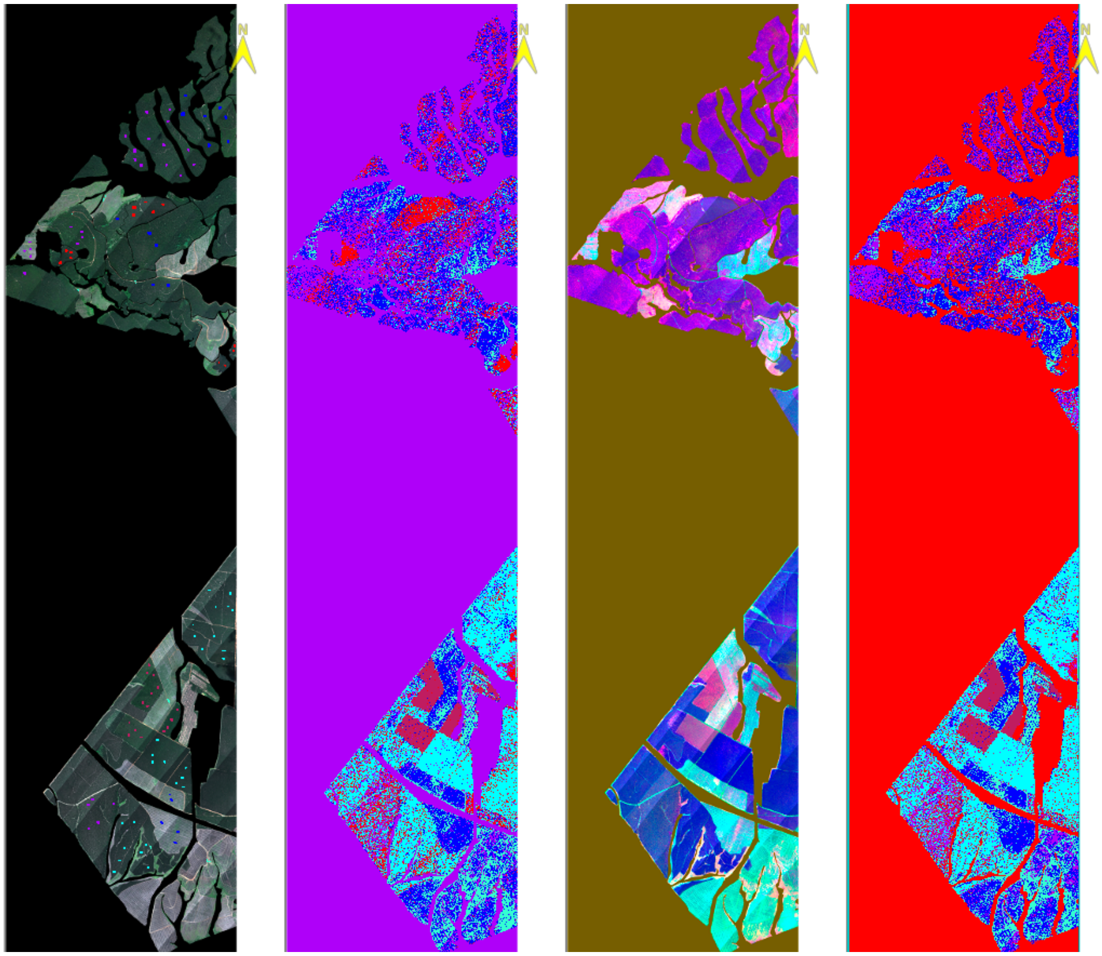

Fig. 3: Classification results: From left to right—Raw data with training samples, classified image using raw data, MNF-reduced data, and classified image using MNF-reduced data. (**Classes**- *Red: GraNit, Blue: Gran, cyan: BS, Teal: Dun, Pastel-Red: Amea*)

TABLE I: Classification accuracy results for raw and MNF-based classifications.

Class	**Raw Classification**		**MNF Classification**	
	Producer's Acc. (%)	**User's Acc (%)**	**Producer's Acc. (%)**	**User's Acc. (%)**
GranNit	84.29	67.08	81.17	59.71
Gran	46.26	61.13	48.30	63.42
Dun	90.47	78.87	93.57	85.45
AMea	95.18	84.97	96.11	87.96
OtherTree	36.96	49.16	39.72	55.18
BS	97.67	93.33	98.29	94.63
	Overall Acc. = 70.10%, Kappa Coeff = 0.63		*Overall Acc. = 71.28%, Kappa Coeff = 0.65*	

The classification of Bare soil is distinct as its spectrum is much different then others. However the classification of vegetation species is not subtle and is mixed. The mixing is because SAM works by setting a threshold level below which all the species are assigned to same class. Since the vegetation spectra detected as end-members arent quite different they have a similar SAM score thus mixed with each other in classification. This method is not quite sufficient for such classification tasks but it can be used as an initial step in getting idea about spectral differences present in the imagery. MLE is far better with distinct boundaries in classification than this method for classification.

IV. Discussion and Conclusion

Species level classification of forest is involves identifying and mapping tree species of interest which is crucial for forest management, biodiversity assessment and other ecological studies and policy design. Airborne hyperspectral imaging has been proven to be a reliable source for such classification due to its ability to capture detailed spectrum of species within a pixel with a large coverage area. We used a Maximum Likelihood Estimation (MLE) based classification routine on

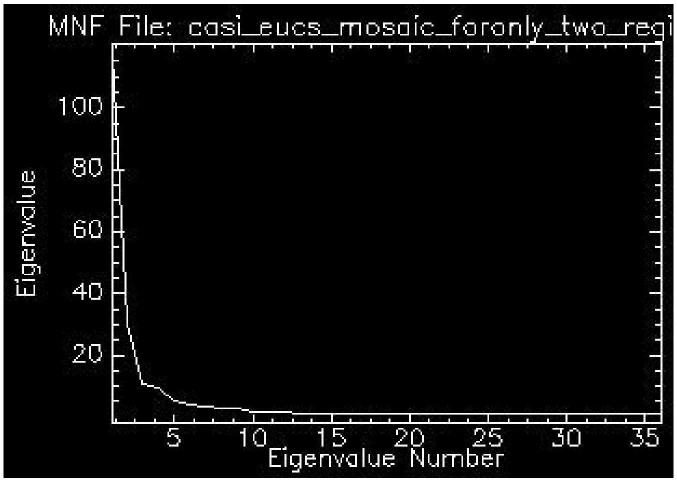

Fig. 4: Band variability plot

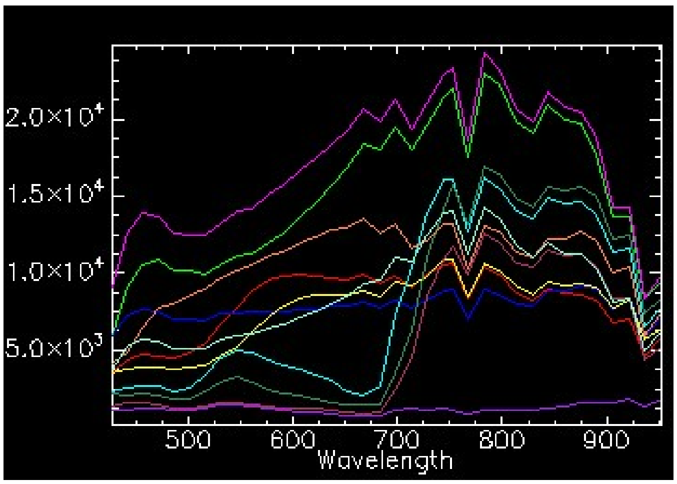

Fig. 5: PPI based end members

a 36 bands hyperspectral data to classify 6 forest classes (4 species and 2 other) applied on raw as well as Maximum Noise Fraction (MNF) reduced data. In general the results in both cases were good considering the resources required to survey such a large area. Most of the classes were easily separable by the algorithm except the one with close resemblance *(Gran and GraNit)*. Overall accuracy was around 70% and Kappa Coefficient was around 65% for both methods, which is still quite good for management purpose, since such tasks don't need a highly accurate classification in general unless the resources are critical. The "Advanced" spectral hourglass wizard tool as compared with MLE based classification didn't give a good result and was able to separate only those classes with clear distinction between spectra *(Veg vs Soil)*, however there was a high confusion among vegetation species due to their high spectral similarity. To conclude, hyperspectral imagery based species classification can provide an efficient tool for managing forest resources over a regional scale.

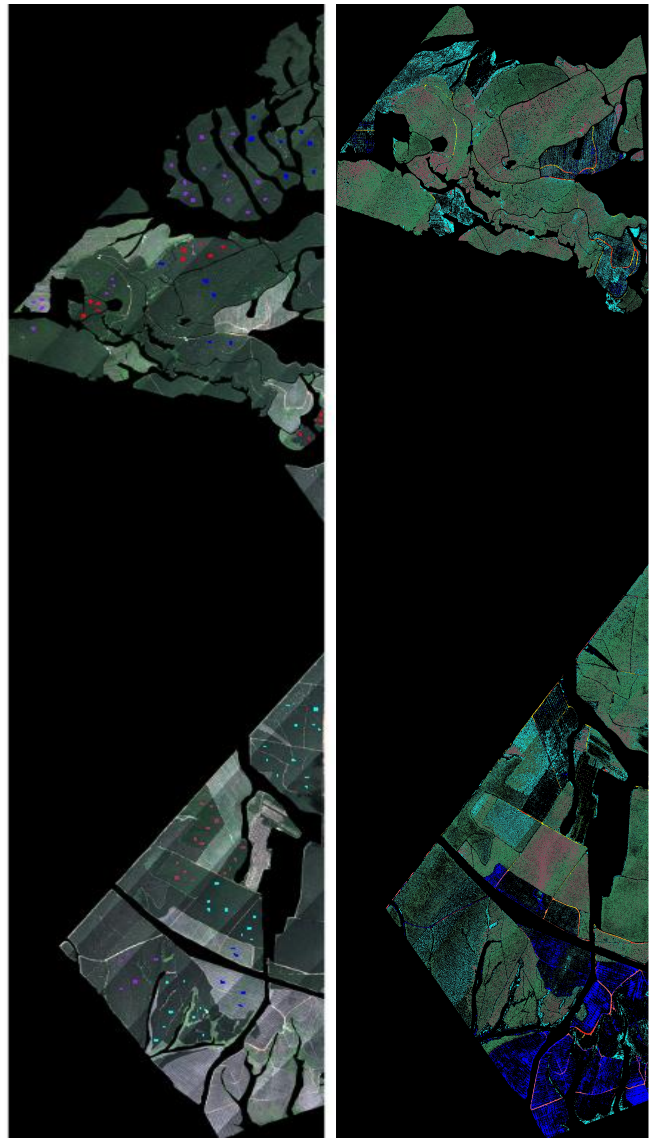

Fig. 6: Comparison of RGB image (left) and SAM output from spectral hourglass wizard (right).
Actual Classes- *Red: GraNit, Blue: Gran, cyan: BS, Teal: Dun, Pastel-Red: Amea*

References

[1] S. E. Franklin, *Remote sensing for sustainable forest management*. CRC press, 2001.

[2] K. Y. Peerbhay, O. Mutanga, and R. Ismail, "Investigating the capability of few strategically placed worldview-2 multispectral bands to discriminate forest species in kwazulu-natal, south africa," *IEEE Journal of Selected Topics in Applied Earth Observations and Remote Sensing*, vol. 7, pp. 307–316, 2014. [Online]. Available: https://api.semanticscholar.org/CorpusID:34338043

[3] T. Hycza, K. Stereńczak, and R. Bałazy, "Potential use of hyperspectral data to classify forest tree species," *New Zealand Journal of Forestry Science*, vol. 48, p. 18, 2018.

[4] M. Michałowska and J. Rapiński, "A review of tree species classification based on airborne lidar data and applied classifiers," *Remote Sensing*, vol. 13, no. 3, 2021. [Online]. Available: https://www.mdpi.com/2072-4292/13/3/353

[5] A. Udali, E. Lingua, and H. J. Persson, "Assessing forest type and tree species classification using sentinel-1 c-band sar data in southern sweden," *Remote Sensing*, vol. 13, no. 16, 2021. [Online]. Available: https://www.mdpi.com/2072-4292/13/16/3237

[6] J. Holmgren, Å. Persson, and U. Söderman, “Species identification of individual trees by combining high resolution lidar data with multi-spectral images,” *International Journal of Remote Sensing*, vol. 29, no. 5, pp. 1537–1552, 2008.

[7] H. Zhu, W. Song, B. Zhang, E. Lu, J. Dai, W. Zhao, and Z. Hu, “Studying forest species classification methods by combining polsar and vegetation spectral indices,” *Forests*, vol. 16, no. 1, 2025. [Online]. Available: https://www.mdpi.com/1999-4907/16/1/15

[8] P. Shippert *et al.*, “Why use hyperspectral imagery?” *Photogrammetric engineering and remote sensing*, vol. 70, no. 4, pp. 377–396, 2004.

[9] F. Melgani and L. Bruzzone, “Classification of hyperspectral remote sensing images with support vector machines,” *IEEE Transactions on geoscience and remote sensing*, vol. 42, no. 8, pp. 1778–1790, 2004.

[10] J.-z. Wu, W.-d. Yan, W.-p. Ni, and H. Bian, “Feature extraction for hyperspectral data based on mnf and singular value decomposition,” in *2013 IEEE International Geoscience and Remote Sensing Symposium - IGARSS*, 2013, pp. 1430–1433.

[11] M. Wilson, S. Ustin, and D. Rocke, “Classification of contamination in salt marsh plants using hyperspectral reflectance,” *IEEE Transactions on Geoscience and Remote Sensing*, vol. 42, no. 5, pp. 1088–1095, 2004.

[12] S. Chakravarty, B. K. Paikaray, R. Mishra, and S. Dash, “Hyperspectral image classification using spectral angle mapper,” in *2021 IEEE International Women in Engineering (WIE) Conference on Electrical and Computer Engineering (WIECON-ECE)*, 2021, pp. 87–90.

[13] Wikipedia contributors, “Softmax function — Wikipedia, the free encyclopedia,” 2025, [Online; accessed 8-February-2025]. [Online]. Available: https://en.wikipedia.org/w/index.php?title=Softmax_function&oldid=1273599451

[14] C.-I. Chang and A. Plaza, “A fast iterative algorithm for implementation of pixel purity index,” *IEEE Geoscience and Remote Sensing Letters*, vol. 3, no. 1, pp. 63–67, 2006.